A new approach to analytical and numerical solutions for nonlinear viscoelastic fluids

Sajjad Pashazadeh and Azadeh Jafari

School of Mechanical Engineering, College of Engineering, University of Tehran, P.O. Box 11155-4563, Tehran, Iran

ABSTRACT

This study provides a new approach for deriving analytical and numerical solutions for finitely extensible nonlinear elastic fluids using the Peterlin closure (FENE-P) viscoelastic fluid flows in a 2D channel and a 3D pipe in a fully developed condition. The validity of the present approach has been confirmed by the analytical solution proposed originally by Cruz et al. (Cruz et al., JNNFM, 132 (2005) 28–35). The numerical simulation of the FENE-P fluid in a slit flow and a tube flow has been carried out using both the spectral/hp element method and the third-order Adams-Bashforth method for the spatial and time discretization respectively. A velocity correction splitting scheme method has been applied for the pressure-velocity decoupling algorithms. The effects of the dimensionless parameter characterizing the viscoelasticity, the Weissenberg number, and the finite extensible parameter are investigated on polymeric normal stress, shear stresses and the velocity profile. Regarding the shear thinning characteristic of the FENE-P model, the velocity profile becomes flatter as Weissenberg number increases.

INTRODUCTION

Nowadays one of the challenges for rheologists is to find and develop analytical and numerical solutions for viscoelastic flow problems. Many analytical and numerical attempts have been made to solve these problems

For many generalized Newtonian fluids, there are analytical solutions derived and compiled by Bird et al.[1]. For some differential viscoelastic models such as the Giesekus and Johnson-Segelmant models, some proposed solutions are available from other researchers; a non-exhaustive list of those research works are[2,3,4,5]. Recently, Cruz et al.[6] have presented analytical solutions for fully developed pipe and channel flows of two viscoelastic fluids including a Newtonian solvent; polymer's contribution is described by Phan Thien Tanner and FENE-P models.

In addition to the analytical solutions for viscoelastic fluid flows, there are a lot of approximate solutions that use different numerical methods. Here, we suffice to say that those research works have used high order numerical methods, specifically spectral element methods (SEMs). Gervang et al.[7] study the viscoelastic flow past a sphere by spectral methods. Fiétier et al.[8] present time-dependent algorithms to develop spectral element methods to simulate unsteady flows of viscoelastic fluids using a closed form of a differential constitutive equation on a straight channel and a 4-1 contraction by UCM and FENE-P models. Fiétier et al.[9] analyze linear stability on time-dependent with SEM by alternating different parameters, factors and boundaries. Phillips et al.[10] employ SEM to simulate viscoelastic flows using Brownian configuration fields; comparisons are made between simulations based on both the Oldroyd-B constitutive model and those based on Brownian configuration fields using Hookean dumbbell models. Jafari et al.[11] propose a new extended matrix logarithm formulation in order to remove instabilities observed in the simulation of unsteady viscoelastic fluid flows (FENE-P model) in the framework of the spectral element method on a 2D channel geometry. Kynch et al.[12] present a high-resolution spectral element approximation of viscoelastic flows (Oldroyd-B and FENE-P) in asymmetric geometries (flows past a fixed sphere) using a DEVSS-G/DG formulation.

This article is divided into two main parts. In the first part, we introduce a new semi-analytical solution for the FENE-P model in a channel and pipe flows in the fully developed condition. In the second part, a numerical solution in the context of SEMs is developed and discussed making a comparison between the proposed analytical solution and the approximate solution of SEM.

GOVERNING EQUATIONS

Figure 1 a and b, below, presents a schematic of the 2D channel and the 3D pipe showing the geometries of this study:

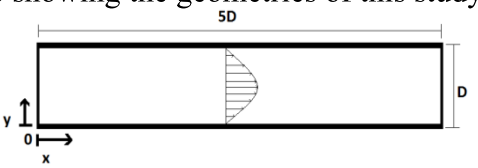

Fig. 1 a. Schematic of the 2D channel

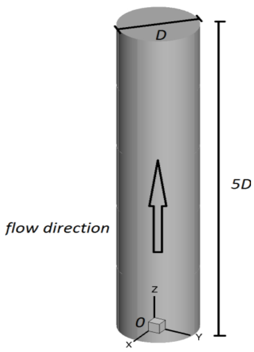

Fig. 1 b. Schematic of the 3D pipe

As in Newtonian flows, the viscoelastic flows are governed by mass and momentum equations. The only difference is that, the momentum equation is modified with respect to the polymeric stresses. For incompressible fluids with constant viscosity, the continuity and momentum equations with respect to viscoelastic fluids can be written as equations (1) and (2) below:

$$\nabla.\boldsymbol{V} = 0, \tag{1}$$

and,

$$\frac{D\boldsymbol{V}}{Dt} = -\frac{1}{\rho}\nabla p + \mu_s \nabla^2 \boldsymbol{V} + \mu_t \nabla.\boldsymbol{\tau_p}, \tag{2}$$

where $\boldsymbol{V}$, $\boldsymbol{\tau_p}$ and p are the velocity and pressure fields, respectively. μ_s, μ_p and ρ show the solvent viscosity, the polymeric viscosity and the density of the fluid, respectively; and $\frac{D\boldsymbol{V}}{Dt}$ is the material derivative function and can be written as:

$$\frac{D\boldsymbol{V}}{Dt} = \frac{\partial \boldsymbol{V}}{\partial t} + \boldsymbol{V}.\nabla\boldsymbol{V} \tag{3}$$

As we have seen in equation (2), the polymeric stresses are added as a source term to the momentum equation in the form of $\nabla.\tau_p$. To obtain the polymeric stresses, a constitutive equation with regards to the viscoelastic model must be calculated. In this study, we work specifically on FENE-P fluids and the mathematical equation of this non-linear dumbbell model will be introduced later.

In order to reduce the parameters that govern our study and decrease the calculation space, and considering repetitive parameters such as specific velocity, U, the height of the channel or diameter of the pipe, D, the density of the fluid, ρ, and the viscosity of the solvent μ_s, we are able to introduce the following dimensionless variables:

$$x_i^* = \frac{x_i}{D} \ , y_i^* = \frac{y_i}{D} \ , t^* = t\frac{U}{D} \tag{4}$$

$$u^* = \frac{u}{U} \ , v^* = \frac{v}{U} \ , P^* = \frac{P}{\rho U^2}$$

$$\tau p_{ij}^* = \frac{\tau p_{ij}}{\mu_s U} \ , C_{ij}^* = \frac{C_{ij}}{\mu_s U}$$

All variables with "*" are in the dimensionless form. For simplicity from now on we omit "*", as all of the variables are converted to the dimensionless form. The dimensionless form of the continuity and momentum equations are as follows:

$$\nabla.\boldsymbol{V} = 0, \text{ and} \tag{5}$$

$$\frac{D\boldsymbol{V}}{Dt} = -\frac{1}{Re}\nabla p + \frac{R_n}{Re}\nabla^2\boldsymbol{V} + \frac{1-R_n}{Re}\nabla.\frac{\boldsymbol{\tau_p}}{Wi} \tag{6}$$

where Re, is the Reynolds number and is equal to the ratio of the inertia forces on the viscous forces. R_n is the ratio of the solvent viscosity to the total viscosity and is equal to $\frac{\mu_s}{\mu_t}$ where $\mu_t = \mu_s + \mu_p$. Finally, Wi is the Weissenberg number and is equal to $\frac{\lambda U}{D}$ and λ is the characteristic relaxation time of the viscoelastic fluids.

it is worth mentioning that for a semi-analytical solution to the pipe flow, we use the cylindrical coordinate, and for the full numerical solution we use the Cartesian coordinate. In the cylindrical coordinate the velocity field is equal to $\boldsymbol{V} = (V_r, V_\theta, V_z)$, where V_r, V_θ, and V_z represents the component of the velocity in the r, θ, z direction and in the Cartesian coordinate, the velocity is equal to $\boldsymbol{V} = (V_x, V_y, V_z)$ and V_x, V_y and V_z are the velocity components in the direction of $x, y, and\ z$ respectively. For the 2D channel, we use the Cartesian coordinate for both the semi-analytical and the full numerical solution, and the velocity vector is defined as $\boldsymbol{V}=(V_x, V_y)$ where V_x and V_y are velocity components in the directions of x, y, respectively. The polymeric stresses for the FENE-P fluid are governed by equation (7),

$$\boldsymbol{\tau_p} = \frac{\boldsymbol{C}}{1-\frac{tr\,(\boldsymbol{C})}{b^2}} - \boldsymbol{I}\,, \tag{7}$$

where b is the finite extensibility parameters; $b = 8$ for this study. $\boldsymbol{C}$ is the conformation tensor and is calculated from the partial differential equation below:

$$\frac{\partial \boldsymbol{C}}{\partial \mathrm{t}} + (\boldsymbol{V}.\nabla)\boldsymbol{C} - (\nabla\boldsymbol{V})^T.\boldsymbol{C} - \boldsymbol{C}.(\nabla\boldsymbol{V}) = -\frac{\boldsymbol{\tau_p}}{Wi}. \tag{8}$$

3D SEMI-ANALYTICAL SOLUTION

To simplify the problem, we assume a fully developed and steady state condition; also, we consider that the velocity in the directions of r and θ is equal to 0 ($V_r = V_\theta = 0$). So, from the continuity equation (5), we have :

$$\nabla.\boldsymbol{V} = \frac{\partial V_r}{\partial r} + \frac{1}{r}\frac{\partial V_\theta}{\partial \theta} + \frac{\partial V_z}{\partial z} = 0 \Rightarrow \frac{\partial V_z}{\partial z} = 0. \tag{9}$$

In order to solve the FENE-P equation (8), we first introduce $\nabla\boldsymbol{V}, \boldsymbol{C}, \boldsymbol{\tau_p}$ in the cylindrical coordinate, as follows:

$$\nabla\boldsymbol{V} = \begin{bmatrix} \frac{\partial V_r}{\partial r} & \frac{\partial V_\theta}{\partial r} & \frac{\partial V_z}{\partial r} \\ \frac{1}{r}\frac{\partial V_r}{\partial \theta} - \frac{V_\theta}{r} & \frac{1}{r}\frac{\partial V_\theta}{\partial \theta} + \frac{V_r}{r} & \frac{1}{r}\frac{\partial V_z}{\partial \theta} \\ \frac{\partial V_r}{\partial z} & \frac{\partial V_\theta}{\partial z} & \frac{\partial V_z}{\partial z} \end{bmatrix} = \begin{bmatrix} 0 & 0 & \frac{\partial V_z}{\partial r} \\ 0 & 0 & 0 \\ 0 & 0 & 0 \end{bmatrix}, \tag{10}$$

$$\boldsymbol{C} = \begin{bmatrix} C_{rr} & C_{r\theta} & C_{rz} \\ C_{r\theta} & C_{\theta\theta} & C_{\theta z} \\ C_{rz} & C_{\theta z} & C_{zz} \end{bmatrix}, \text{ and} \tag{11}$$

$$\boldsymbol{\tau_p} = \begin{bmatrix} \tau_{rr} & \tau_{r\theta} & \tau_{rz} \\ \tau_{r\theta} & \tau_{\theta\theta} & \tau_{\theta z} \\ \tau_{rz} & \tau_{\theta z} & \tau_{zz} \end{bmatrix}. \tag{12}$$

by introducing the above equations (10) to (12), in equation (8), we get:

$$rr\!: \tau_{rr} = 0, r\theta\!: \tau_{r\theta} = 0, \tag{13}$$

$$rz\!: \frac{\tau_{rz}}{Wi} = C_{rr}\frac{\partial V_z}{\partial r}, \theta\theta\!: \tau_{\theta\theta} = 0,$$

$$\theta z\!: \frac{\tau_{\theta z}}{Wi} = C_{r\theta}\frac{\partial V_z}{\partial r},\ zz\!: \frac{\tau_{zz}}{Wi} = 2C_{rz}\frac{\partial V_z}{\partial r}.$$

Extending equation (7) and combining it with equation (13) produces the following:

$$rr\!: \frac{C_{rr}}{1-\frac{tr(C)}{b^2}} - 1 = 0 \ \Rightarrow\ C_{rr} = 1 - \frac{tr(\boldsymbol{C})}{b^2}, \tag{14}$$

$$r\theta\!: \frac{C_{r\theta}}{1-\frac{tr(C)}{b^2}} = 0 \ \Rightarrow\ C_{r\theta} = 0, \tag{15}$$

$$rz\!: \frac{C_{rz}}{1-\frac{tr(C)}{b^2}} = \tau_{rz} = WiC_{rr}\frac{\partial V_z}{\partial r}, \tag{16}$$

$$\theta\theta\!: \frac{C_{\theta\theta}}{1-\frac{tr(C)}{b^2}} - 1 = 0 \ \Rightarrow\ C_{\theta\theta} = 1 - \frac{tr(\boldsymbol{C})}{b^2}, \tag{17}$$

$$\theta z\!: \frac{C_{\theta z}}{1-\frac{tr(C)}{b^2}} = \tau_{\theta z} = WiC_{r\theta}\frac{\partial V_z}{\partial r} \tag{18}$$

$$\overset{(13)}{\Longrightarrow}\ C_{\theta z} = 0, \text{ and}$$

$$zz\!: \frac{C_{zz}}{1-\frac{tr(C)}{b^2}} - 1 = \tau_{zz} = 2WiC_{rz}\frac{\partial V_z}{\partial r}. \tag{19}$$

Next, by extending equation (6), we have:

$$r:\ \frac{\partial p}{\partial r}=0,\theta:\ \frac{\partial p}{\partial \theta}=0,$$

$$z:\ \frac{1}{Re}\frac{\partial p}{\partial z}=\frac{R_n}{Re}\left[\frac{1}{r}\frac{\partial}{\partial r}\left(r\frac{\partial V_z}{\partial r}\right)\right]+\frac{1-R_n}{Re}.\frac{1}{Wi}\left(\frac{\partial \tau_{rz}}{\partial r}+\frac{\tau_{rz}}{r}\right)$$
$$=\frac{R_n}{Re}\left(\frac{1}{r}\frac{\partial V_z}{\partial r}+\frac{\partial^2 V_z}{\partial r^2}\right)+\frac{1-R_n}{Re}.\frac{1}{Wi}\left[\frac{\partial}{\partial r}\left(WiC_{rr}\frac{\partial V_z}{\partial r}\right)+Wi\frac{C_{rr}}{r}\frac{\partial V_z}{\partial r}\right]. \quad (20)$$

In the equation above, due to couplings and the non-linearity of the equation, it is not easy to find a full analytical solution. One of the most accessible ways to reach an analytical solution is by using numerical methods. We use a finite difference with first order backward discreet domain into 1,000 parts, and explicitly by the boundary of no-slip condition on(r=R);therefore, we can find a solution for the $V_z, \boldsymbol{C}$ terms and subsequently find $\boldsymbol{\tau_p}$ by equation (13) relations.

2D SEMI-ANALYTICAL SOLUTIONS

For 2D geometry, in the Cartesian coordinate and assuming that $V_y=0$, the continuity equation will be simplified to:

$$\nabla.V=\frac{\partial V_x}{\partial x}+\frac{\partial V_y}{\partial y}=\frac{\partial V_x}{\partial x}=0, \quad (21)$$

and the gradient of the velocity field, the conformation tensor, and the polymeric stresses in the 2D Cartesian coordinate can be written as:

$$\nabla\boldsymbol{V}=\begin{bmatrix}\frac{\partial V_x}{\partial x} & \frac{\partial V_x}{\partial y}\\ \frac{\partial V_y}{\partial x} & \frac{\partial V_y}{\partial y}\end{bmatrix}=\begin{bmatrix}0 & \frac{\partial V_x}{\partial y}\\ 0 & 0\end{bmatrix}, \quad (22)$$

$$\boldsymbol{C}=\begin{bmatrix}C_{xx} & C_{xy}\\ C_{xy} & C_{yy}\end{bmatrix}, \text{ and} \quad (23)$$

$$\boldsymbol{\tau_p}=\begin{bmatrix}\tau_{xx} & \tau_{xy}\\ \tau_{xy} & \tau_{yy}\end{bmatrix}. \quad (24)$$

Introducing equations. (22) to (24) into equation (8) produces:

$$\tau_{xx}=2WiC_{xy}\frac{\partial V_x}{\partial y}, \quad (25)$$

$$\tau_{xy}=WiC_{yy}\frac{\partial V_x}{\partial y}, \text{and} \quad (26)$$

$$\tau_{yy}=0. \quad (27)$$

From equation (6) we get :

$$\frac{\partial p}{\partial x}=\frac{R_n}{Re}\frac{\partial^2 V_x}{\partial y^2}+\frac{1-R_n}{ReWi}\frac{\partial \tau_{xy}}{\partial y}, \text{and} \quad (28)$$

$$\frac{\partial p}{\partial y}=0. \quad (29)$$

by integrating equation (28) in the y-direction and implementing the boundary condition in the center of the channel $\left(\frac{\partial V_x}{\partial y}=\tau_{xy}=0, at: y=\frac{D}{2}\right)$, we have:

$$\frac{\partial V_x}{\partial y}=-\frac{1-R_n}{R_nWi}\tau_{xy}+\frac{Re\frac{\partial p}{\partial x}}{R_n}y-\frac{Re\frac{\partial p}{\partial x}}{R_n}\frac{D}{2}. \quad (30)$$

Then, by combining equations (26) and (30), we reach the relationship as follows:

$$\frac{\partial V_x}{\partial y}=\frac{R_n}{R_n+C_{yy}-R_nC_{yy}}\left(\frac{Re\frac{\partial p}{\partial x}}{R_n}y-\frac{Re\frac{\partial p}{\partial x}}{2R_n}D\right). \quad (31)$$

By coupling equation (7) with equations (27), (26) and (25) respectively we have:

$$C_{yy}=1-\frac{tr(c)}{b^2}=\frac{b^2-C_{xx}}{1+b^2}, \quad (32)$$

$$\frac{C_{xy}}{1-\frac{tr(c)}{b^2}}=WiC_{yy}\frac{\partial V_x}{\partial y}, \text{and} \quad (33)$$

$$\frac{C_{xx}}{1-\frac{tr(c)}{b^2}}-1=2WiC_{xy}\frac{\partial V_x}{\partial y}. \quad (34)$$

Finally, by solving the system of equations (31) to (34), it is possible to find a solution for $\frac{\partial V_x}{\partial y}$ and subsequently for τ_{xx}, τ_{xy}. In order to find the velocity, we integrate equation (30) in the direction of y, as follows:

$$V_x=-\frac{1-R_n}{R_nWi}\int\tau_{xy}dy+\frac{Re\frac{\partial p}{\partial x}}{2R_n}y^2-\frac{Re\frac{\partial p}{\partial x}}{R_n}\frac{D}{2}y. \quad (35)$$

SPECTRAL ELEMENT METHOD

Spectral methods are estimated by high order polynomials approximation (usually according to Chebyshev). We usually use this method in simple geometries as it is not easy to manipulate in complex geometry, except by using the decomposition method; that finally leads to some of the complicated equations taught. Spectral element methods, or SEM, is a mixture of finite element method capability in complex geometries with high order polynomials, precise approximation of spectral methods. The difficulty of implementing SEM is balanced by its great and fascinating capability to reach solutions in the areas that have high gradient and lower dissipation and distortion compared to other numerical methods. This method had been used in [13-15]. The spectral/hp element method includes refinement with two techniques, "p" and "h"; "p" refers to the number of elements, and "h" refers to the polynomials degree in approximations. By increasing the number of elements and degrees we are able increase develop the accuracy of solutions. The domain in the 2D channel was divided into 20 equal elements, and the 3D cylinder was also divided into 20 elements. The discrete geometries are shown in Figure 2, below.

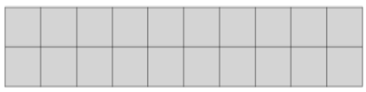

a) Spectral element of a 2D channel

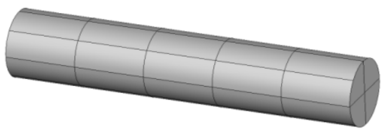

b) Spectral element of a 3D pipe

Fig. 2. Discrete geometries

Each dependent parameter, such as the pressure, tension and velocity on the standard element through the expansion of tonsorial basis, is approximated as follows:

for 2D channel we have:

$$\psi(\xi_1,\xi_2) \approx \sum_{p=0}^{N} \sum_{q=0}^{N} \Phi_p(\xi_1)\Phi_q(\xi_2)\hat{\psi}_{pq} \tag{36}$$

, and for 3D pipe we have:

$$\psi(\xi_1,\xi_2,\xi_3) \approx \sum_{p=0}^{N} \sum_{q=0}^{N} \sum_{s=0}^{N} \Phi_p(\xi_1)\Phi_q(\xi_2)\Phi_s(\xi_3)\hat{\psi}_{pqs} \tag{37}$$

where ψ is the general dependent term; $\hat{\psi}_{pqs}$, $\hat{\psi}_{pq}$ are the expansion coefficients; ξ_i are the local spatial alternatives that are put in -1, +1; N is the degree of basis; and finally, Φ_p, Φ_q, Φ_s are modal functions that could be calculated as follows:

$$\Phi_j = \begin{cases} \frac{(1-\xi)}{2} & j = 0 \\ \frac{(1-\xi)}{2}\frac{(1+\xi)}{2}\mathbf{P}_{j-1}^{1,1}(\xi) & for\ 0 < j < N, \\ \frac{(1+\xi)}{2} & j > N \end{cases} \tag{38}$$

where $\mathbf{P}_{j-1}^{1,1}$ is a Jacobi function [16]. Also to discretize the time aspect of the problem in, we use the 3rd order of Adams Bashforth method; for more information please refer to [17].

The numerical study in both the 2D and 3D test cases was carried out using $dt = 10e - 05$ and the polynomial degree of the modal basis in all space directions was set to $N = 5$.

BOUNDARY CONDITIONS

For the 2D channel:

	Inlet	Outlet	Walls
Polymeric Tensions	Dirichlet : (our semi-analytical solution)	Neumann: (fully developed)	Dirichlet: (our semi-analytical solution)
Velocity	Dirichlet : (our semi-analytical solution)	Neumann: (fully developed)	Dirichlet: (no-slip condition)
Pressure	Neumann: (fixed gradient)	Dirichlet: (zero pressure)	Neumann : (zero)

For the 3D pipe, we used the same boundary condition; however, for the pressure on the walls and outlet we used high order boundary condition. For more information please refer to [18].

RESULTS

All the parameters set in our study are equal to:

$$Re = 1\,, b = 8\,, D = 1\,, Rn = \frac{1}{9} \tag{39}$$
$$\frac{\partial p}{\partial x} = -0.11(for\ 2D)\ , \quad \frac{\partial p}{\partial z} = -0.11(for\ 3D)$$

To validate our analytical solutions, we compared our results with the analytical result proposed by Cruz et al. [6] in both geometries. Figure 3, below, shows the polymeric normal and shear stresses and the velocity profile at $Wi = 5$ for the 2D channel at the outlet's cross-section.

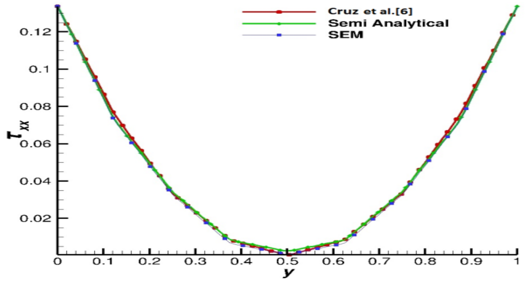

a)

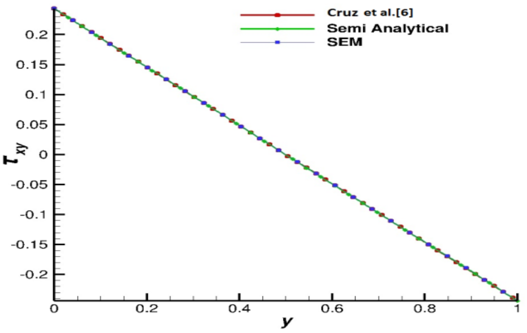

b)

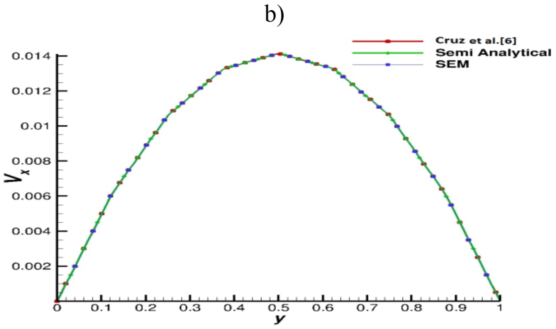

c)

Fig. 3. 2D validation at the exit of the channel. a) Normal stress b) Shear stress c) Stream-wise velocity

As can be seen in Fig3, the present semi-analytical solution and the numerical solution have very good agreement with the analytical solution of Cruz et al.[6]. The polymeric normal and shear stresses with stream-wise velocity and pressure along the channel at $Wi = 5$ are shown in Figure 4.

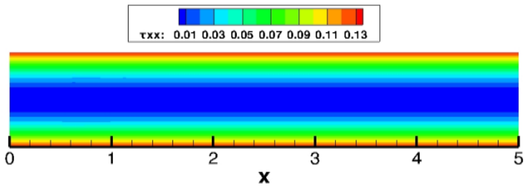

a) Polymeric normal stress

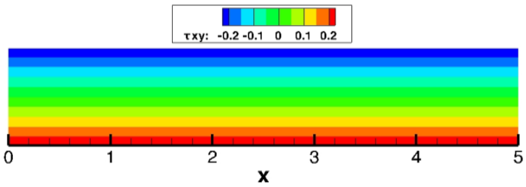

b) Polymeric shear stress

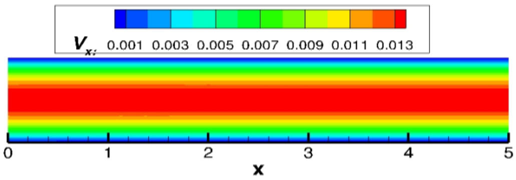

c) Stream-wise velocity

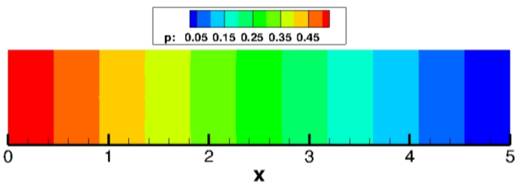

d) Pressure

Fig. 4. Numerical solution of FENE-P fluids at $Wi = 5$ in the channel flow. a) Polymeric normal stress, b) Polymeric shear stress, c) Stream-wise velocity, d) Pressure.

Figure 5, represents the comparison of the present analytical and numerical solution with the analytical solution proposed by Cruz et al. [6] in the 3D pipe. Similar to the 2D geometry, a very good agreement for all variables, polymeric normal stress, shear stresses, and stream-wise velocity can be seen see in Figure 5.

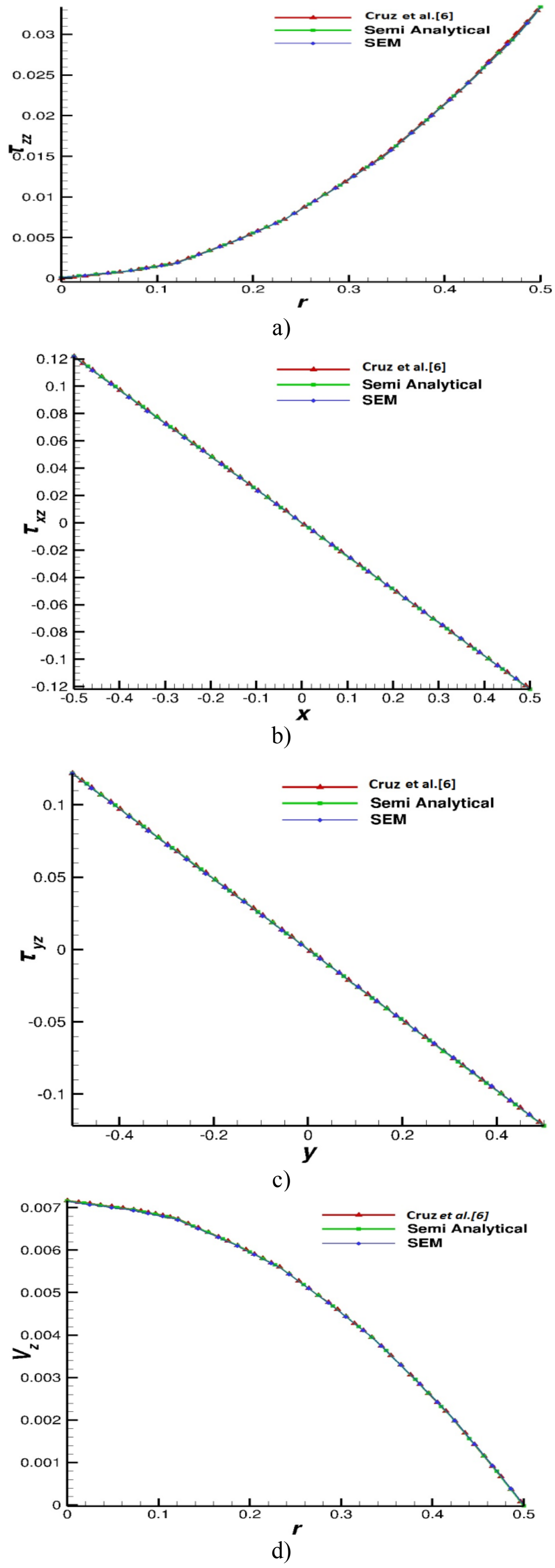

Fig. 5. Validation of the pipe flow. a) Normal stress. b) Shear stress in x-direction. c)Shear stress in y-direction. d)Axial velocity

The numerical results of the contours of the polymeric stresses, velocity, and pressure are shown in Figure 6, below.

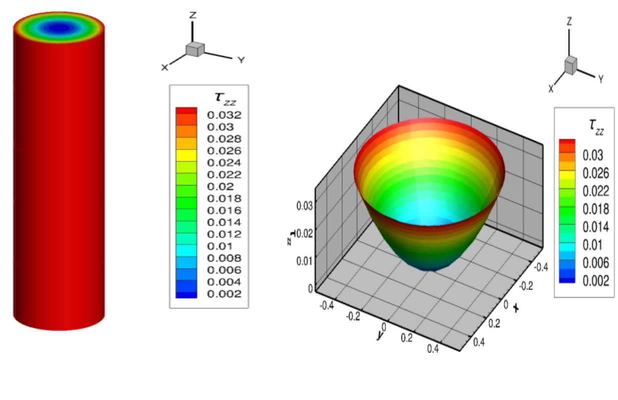

a) Polymeric normal stress

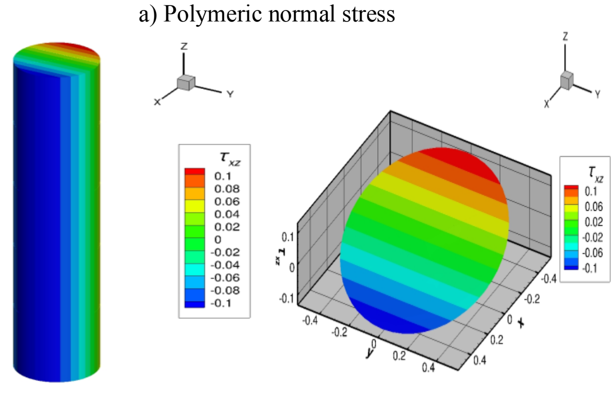

b) Polymeric shear stress in the x-direction

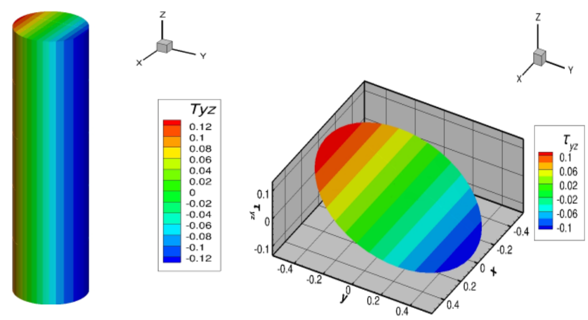

c) Polymeric shear stress in the y-direction

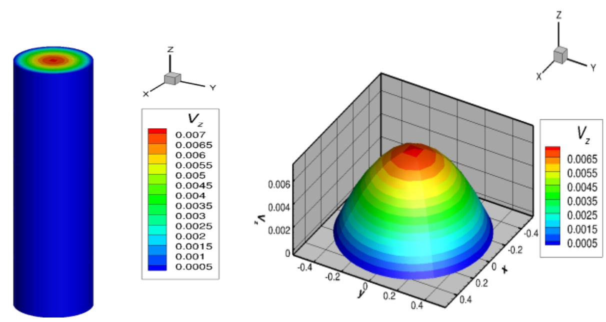

d) Stream-wise velocity

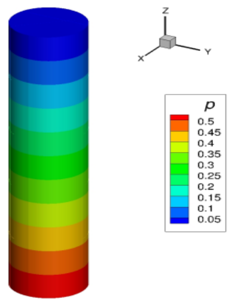

e)Pressure

Fig. 6. Numerical solution of FENE-P fluids at $Wi = 5$ in the pipe flow. a) Polymeric normal stress, b) Polymeric shear stress in the x-direction, c) Polymeric shear stress in the y-direction, d) Stream-wise velocity e) Pressure

CONCLUSION

In this paper, we propose a new methodology to obtain a semi-analytical solution for the FENE-P fluids in a 2D channel and a 3D pipe flow. As part of the analytical solution, we simulated the 2D and 3D flows using spectral element methods. The validations of the present analytical and numerical solutions were carried out by making comparisons with the analytical solution originally proposed by Cruz et al. [6]. Both the numerical and analytical results show very good agreement with the analytical result of Cruz et al. for both the 2D and 3D fluid flows.

ACKNOWLEDGMENTS

The support of the Computational non-Newtonian Fluid mechanic Laboratory, cnnfm.ut.ac.ir, is gratefully acknowledged.

REFERENCES

1. Bird, R.B., R.C. Armstrong, and O. Hassager, *Dynamics of polymeric liquids. Vol. 1: Fluid mechanics.* 1987.

2. Johnson Jr, M. and D. Segalman, A model for viscoelastic fluid behavior which allows non-affine deformation. *Journal of Non-Newtonian Fluid Mechanics*, 1977. **2**(3): p. 255-270.

3. Van Schaftingen, J. and M. Crochet, Analytical and numerical solution of the Poiseuille flow of a Johnson-Segalman fluid. *Journal of Non-Newtonian Fluid Mechanics*, 1985. **18**(3): p. 335-351.

4. Yoo, J. and H.C. Choi, On the steady simple shear flows of the one-mode Giesekus fluid. *Rheologica Acta*, 1989. **28**(1): p. 13-24.

5. Schleiniger, G. and R.J. Weinacht, Steady Poiseuille flows for a Giesekus fluid. *Journal of Non-Newtonian Fluid Mechanics*, 1991. **40**(1): p. 79-102.

6. Cruz, D., F.T.d. Pinho, and P.J. Oliveira, Analytical solutions for fully developed laminar flow of some viscoelastic liquids with a Newtonian solvent contribution. *Journal of Non-Newtonian Fluid Mechanics*, 2005. **132**(1-3): p. 28-35.

7. Gervang, B., A. Davies, and T. Phillips, On the simulation of viscoelastic flow past a sphere using spectral methods. *Journal of Non-Newtonian Fluid Mechanics*, 1992. **44**: p. 281-306.

8. Fiétier, N. and M.O. Deville, Time-dependent algorithms for the simulation of viscoelastic flows with spectral element methods: applications and stability. *Journal of Computational Physics*, 2003. **186**(1): p. 93-121.

9. Fiétier, N. and M.O. Deville, Linear stability analysis of time-dependent algorithms with spectral element methods for the simulation of viscoelastic flows. *Journal of Non-Newtonian Fluid Mechanics*, 2003. **115**(2-3): p. 157-190.

10. Phillips, T. and K. Smith, A spectral element approach to the simulation of viscoelastic flows using Brownian configuration fields. *Journal of Non-Newtonian Fluid Mechanics*, 2006. **138**(2-3): p. 98-110.

11. Jafari, A., N. Fiétier, and M.O. Deville, A new extended matrix logarithm formulation for the simulation of

viscoelastic fluids by spectral elements. *Computers & Fluids*, 2010. **39**(9): p. 1425-1438.

12. Kynch, R. and T. Phillips, A high resolution spectral element approximation of viscoelastic flows in asymmetric geometries using a DEVSS-G/DG formulation. *Journal of Non-Newtonian Fluid Mechanics*, 2017. **240**: p. 15-33.
13. Wei, C., D. Gottlieb, and A. Harten, *Cell averaging Chebyshev methods for hyperbolic problems. Final report*. 1990, National Aeronautics and Space Administration.
14. McDonald, B., Flux-corrected pseudospectral method for scalar hyperbolic conservation laws. *Journal of Computational Physics*, 1989. **82**(2): p. 413-428.
15. Sherwin, S. and G.E. Karniadakis, A triangular spectral element method; applications to the incompressible Navier-Stokes equations. *Computer methods in applied mechanics and engineering*, 1995. **123**(1-4): p. 189-229.
16. Karniadakis, G.E. and S.J. Sherwin, *Spectral/hp element methods for CFD (Numerical mathematics and scientific computation)*. 1999: Oxford University Press, New York.
17. Gear, C.W., *Numerical initial value problems in ordinary differential equations*. 1971: Prentice Hall PTR.
18. Karniadakis, G.E., M. Israeli, and S.A. Orszag, High-order splitting methods for the incompressible Navier-Stokes equations. *Journal of Computational Physics*, 1991. **97**(2): p. 414-443.
19. Jafari, A., et al., Property preserving reformulation of constitutive laws for the conformation tensor. *Theoretical and Computational Fluid Dynamics*, 2018. **32**(6): p. 789-803.